Projection-Based Phase Features for Localization of a Needle Tip in 2D Curvilinear Ultrasound

Ilker Hacihaliloglu[1], Parmida Beigi[1], Gary Ng[3], Robert N. Rohling[1,2], Septimiu Salcudean[1], and Purang Abolmaesumi[1]

[1] Electrical and Computer Engineering, University of British Columbia, Canada
[2] Mechanical Engineering, Universtiy of British Columbia, Canada
[3] Philips Research, Bothell, Washington, United States

Abstract. Localization of a needle's tip in ultrasound images is often a challenge during percutaneous procedures due to the inherent limitations of ultrasound imaging. A new method is proposed for tip localization with curvilinear arrays using local image statistics over a region extended from the partially visible needle shaft. First, local phase-based image projections are extracted using orientation-tuned Log-Gabor filters to coarsely estimate the needle trajectory. The trajectory estimation is then improved using a best fit iterative method. To account for the typically discontinuous needle shaft appearance, a geometric optimization is then performed that connects the extracted inliers of the point cloud. In the final stage, the enhanced needle trajectory points are passed to a feature extraction method that uses a combination of spatially distributed image statistics to enhance the needle tip. The needle tip is localized using the enhanced images and calculated trajectory. Validation results obtained from 150 *ex vivo* ultrasound scans show an accuracy of 0.43 ± 0.31 mm for needle tip localization.

Keywords: Ultrasound, local phase, epidurals, needle enhancement.

1 Introduction

Ultrasound (US) guidance is useful for many needle insertions, including biopsy, therapy and anesthesia. The key is to observe the advancement of a needle tip towards the target. Unfortunately, needle visualization in US images is strongly dependent on the orientation of the specularly reflecting needle to the US beam and is poorest when performing blocks with a steep needle insertion angle, such as, typically femoral blocks in obese patients [1]. Medium frequency curvilinear transducers are used to achieve the necessary depth of penetration and field of view, but only a small portion or none of the needle gives a strong reflection. Needle visibility can be successfully enhanced by beam steering on linear transducers, seen on commercial machines, but only a portion of the needle is enhanced with curvilinear arrays so the tip is still indistinguishable. A solution

N. Navab et al. (Eds.): MICCAI 2015, Part I, LNCS 9349, pp. 347–354, 2015.
DOI: 10.1007/978-3-319-24553-9_43

is needed for enhancing and localizing a needle in US images obtained using curvilinear transducers.

The following papers provide a brief overview of the general history of needle enhancement in US. Methods based on Radon transform and variants of Hough transform were proposed by different groups [2, 3]. The needle tip localization error results varied between 0.45 mm and 1.92 mm for *ex vivo* or phantom scans. In [2], validation on clinical scans achieved a mean needle targeting error value of 0.19 mm. However, tip localization accuracy was not reported. Parallel integral projection based algorithms, based on the fact that needles appear as the highest intensity line-like features in US images, were used in [4–6]. The reported needle tip localization results on turkey breast [4], gel phantom [5] and *in vivo* animal study [6] were 0.69 mm, 0.26 mm and 1.4 mm respectively. Uhercik *et al.* [7] used intensity thresholding, a robust randomized search procedure using random sample consensus (RANSAC), and tool axes optimization for needle shaft localization. The tissue-mimicking phantom experiment resulted with a mean tip localization accuracy of 0.64 mm. In recent work, Wu *et al.* [8] used gradient orientation and magnitude information for localizing needles. Chicken breast phantom experiments achieved a minimum tip localization error of $<$ 0.85 mm. On *In vivo* patient scans the method achieved a needle tip localization accuracy of 1.15 mm [8].

This paper focuses on the challenge of guiding a needle for epidurals, particularly for lumbar blocks, where the needle shaft is poorly visible due to the steep trajectory and variable strength reflections due to range of beam angles from the curvilinear transducer. Our proposed method for needle trajectory estimation is based on the extraction of local phase needle image projections obtained using orientable Log-Gabor filters. The key innovation for extracting the needle tip, is a new feature extraction method based on the combination of spatially distributed image statistics into a compact feature descriptor using the information extracted from the needle trajectory. We show qualitative and quantitative validation results on *ex vivo* US scans obtained from bovine and porcine tissue samples using a relative needle and transducer geometry suitable for lumbar in-plane US guided needle insertion.

2 Methods

The proposed enhancement method is based on our previous experience with in-plane guidance of lumbar injections *in vivo* where (i) the needle is inserted in-plane and the insertion side (left or right) is known, (ii) the needle tip appears as a characteristic but variable intensity echo, and (iii) only the portion of the needle shaft close to the transducer surface is visible. Specifically, we focus on the enhancement of in-plane needles with mid to steep insertion angles from 2D US images obtained using a curvilinear transducer (Fig. 1 (a)). In this work, we investigate needle insertion angles (α) ranging from 40° to 70°, to the skin surface. Due to the convex shape of the transducer and the mid to steep insertion angle, the only visible part of the needle shaft is the part that is close to the

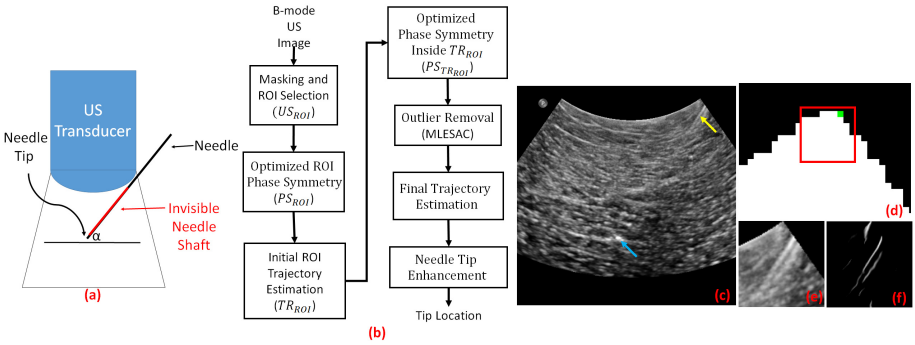

Fig. 1. (a) Schematic drawing of the experimental imaging setup. The insertion angle (α) is measured in relation to the phantom/skin surface ($\alpha = 0°$ is parallel to the skin surface). (b) Flowchart of the proposed method. (c) B-mode US image. The yellow arrow points to the partially visible needle shaft and the blue arrow points the needle tip. (d) Zoom in of the upper right side of the mask image where ROI selected mask image is shown in the red square. (e) B-mode US image corresponding to the selected ROI (US_{ROI}). (f) Optimized local phase image of (e) (PS_{ROI}).

transducer surface where the needle is nearly perpendicular to the US beam (Fig. 1 (c)). In the next section we provide an explanation how these imaging features are used in our proposed method. The flowchart of the proposed method is provided in Fig. 1 (b).

2.1 Needle Tip Localization Using Projection-Based Image Phase Features

Optimized Phase Projections: The first step of the proposed method is to automatically extract a region of interest (ROI) that covers that visible needle section. This is achieved by producing a mask from the B-mode US image using simple thresholding and selecting the pixel that is located on the far right top corner of this mask image (Fig. 1 (d) green pixel). We define our ROI by creating a rectangular region around this pixel where the pixel location is the centre of the top side of the rectangle. The ROI US image will be denoted as US_{ROI} (Fig. 1 (e)). In all the collected scans, the needle was inserted from the right side of the B-mode image. *A priori* knowledge of the needle insertion side is used during this step. Accurate selection of this ROI is not critical for the algorithm; it only needs to contain a portion of the needle shaft.

Recently, intensity-invariant, local phase-based image processing methods, based on filtering the US data with band-pass Log-Gabor filters, have shown promising results for extraction of soft tissue and bone interfaces [9]. Phase-based features are designed to be intensity-invariant and therefore insensitive to US imaging parameters such as imaging depth, as evidenced in previous work on bone detection [9]. In order to extract the needle shaft, we filter the

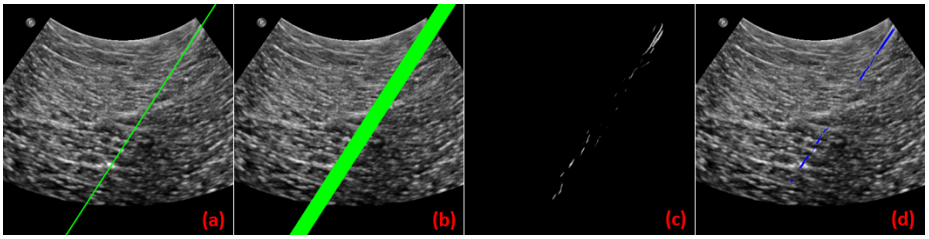

Fig. 2. (a) Estimated initial trajectory (green line) overlaid on the B-mode US image. (b) The extended ROI trajectory(TR_{ROI}) overlaid on the B-mode US image. (c) The $PS_{TR_{ROI}}$ image calculated from the B-mode US image by limiting the local phase feature extraction to the region defined by TR_{ROI}. (d) Inliers detected using the MLESAC algorithm (blue pixels) overlaid on top of the B-mode US image.

US_{ROI} image with a Log-Gabor filter whose transfer function is defined as $LG(\omega,\theta) = exp(\frac{-log(\omega/\kappa)^2}{2log(\sigma_\omega)^2})exp(\frac{-(\theta-\theta_m)^2}{2(\sigma_\theta)^2})$. Here ω and θ are related to the scale and orientation of the filter. κ is the centre frequency of the filter, σ_ω is related to the spread of the frequency spectrum in a logarithmic function, and σ_θ defines the angular bandwidth of the filter. θ_m is the specific orientation of the filter. These filter parameters were selected automatically using the framework proposed by Hacihaliloglu *et al.* [9]. The output of this filtering operation is used to construct a phase-based descriptor called phase symmetry (PS) [9]. The PS_{ROI} image extracted by processing the US_{ROI} image shows a distinct local phase feature for the needle shaft (Fig. 1 (f)).

Initial Trajectory Estimation: In order to estimate the initial trajectory we calculate the Radon Transform (RT) of the PS_{ROI} image. The initial needle trajectory is estimated by performing an inverse RT operation using only the peak RT value (Fig. 2 (a)). In order to account for a possible bending of the needle during the insertion and provide a more accurate initial trajectory estimate, we extend this estimated trajectory to an initial trajectory ROI which we call TR_{ROI}. TR_{ROI} is calculated by keeping the maximum RT and its angle value constant but expanding the corresponding distance (ρ) by $\Delta\rho$ pixels in each direction in the RT space and calculating the inverse RT (Fig. 2 (b)). The diameter of the needle used in this study is 1.47 mm; to select a safe zone we expand this diameter value to 5.47 mm (2 mm from each side) which accounts for a $\Delta\rho$ value of 20 pixels, accommodating common anesthesia needles.

Final Trajectory Estimation: The TR_{ROI}, calculated in the previous step, provides a region in the B-mode US image which includes the needle shaft and tip. To enhance these two features, the local phase-based PS calculation is performed on the full sized US image but by limiting the extraction process to the region defined by TR_{ROI}. We define this new PS image as $PS_{TR_{ROI}}$. Limiting the PS calculation to the TR_{ROI} eliminates the extraction of unwanted soft tissue interfaces and focuses on the ROI where the needle shaft and the tip is expected

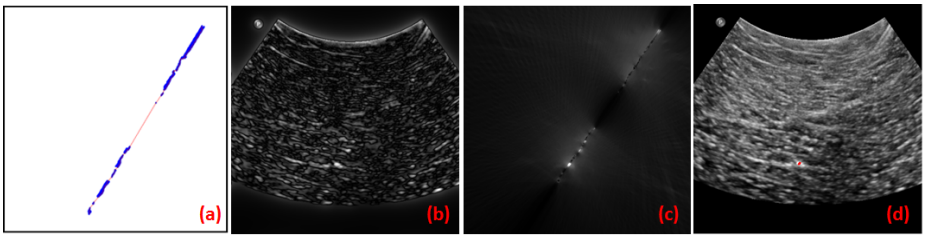

Fig. 3. (a) Final needle trajectory, (shown in red) obtained after geometric optimization approach, overlaid on the disconnected MLESAC point cloud (shown in blue). The line segments 'a','b' and the black circle (knot) are used during the needle tip detection. (b) Band-pass filtered B-mode US image used as input for tip estimation. (c) Output obtained from the needle tip enhancement approach.(d) Enhanced needle tip (shown in red) overlaid on the B-mode US image.

to be (Fig. 2 (c)). Investigating Fig. 2 (c) we can see that there are still some false positive local phase features in the $PS_{TR_{ROI}}$ image. In order to eliminate the final remaining false positive local phase features we perform a randomized search procedure by modifying the traditional RANSAC (Random Sample Consensus) algorithm. The traditional RANSAC approach fits a model the point cloud based on a threshold value. Therefore, the accuracy of the RANSAC algorithm, for needle axis localization, is limited to this selected threshold value [7]. In order to overcome this problem we propose to use a new method called Maximum Likelihood Estimation SAmple Consensus (MLESAC)[10]. MLESAC evaluates the likelihood of the hypothesis, representing the error distribution as a mixture model. The error is modeled as a mixture model of Gaussian and uniform distribution $p(e) = (\gamma(\frac{1}{\sqrt{2\pi}\sigma})exp(-\frac{e^2}{2\sigma^2}) + \frac{(1-\gamma)}{\nu})$. Here ν is the diameter of the search window, γ is the mixing parameter and σ is the standard deviation of the error on each coordinate. The final step is to find the best estimate which minimizes the negative log likelihood of the error function [10] using expectation maximization (EM) algorithm. Parameter γ is estimated during the EM part and ν is dependent on the data size. The MLESAC algorithm results are shown in Figure 2 (d) where we can see a clear overlap of the detected inliers with the needle shaft as well as the needle tip. The final trajectory estimate is obtained by connecting these extracted inliers using a geometric optimization approach [11]. Given a collection of F curves and n inlier points (x_i, y_i), $i = 1, ..., n$, the optimization approach tries to find the size of the largest subset of points $(N_n(F))$ lying on a curve in F. Based on the *a priori* knowledge that the needle shaft is a rigid object and should follow a straight path with minimal bending, we define the curve as a monotonic Lipschitz function. If we define $M(i)$ as the maximum number of points from $(x_1, y_1), ..., (x_i, y_i)$ on a curve ending at (x_i, y_i), during the optimization, we compute $M(i) = 1 + max_{j<i, y_j<y_i} M(j)$ and then $N_n(F) = max[M(i)]$. The estimated final trajectory obtained is shown in Fig. 3 (a) as a red line.

Needle Tip Enhancement and Localization Using Spatially Distributed Image Statistics: The needle tip estimation is based on the RT, but instead of integrating the US image intensity values along a line L, they are distributed among various line segments along L (e.g. Fig. 3 (a) segments 'a' and 'b') [12]. The line segments are defined by a set of salient points, called knots (Fig. 3 (a) black circle), along L which are the intersection points of L and the trajectory estimated in the previous step. By using the trajectory we eliminate the extraction/enhancement of the soft tissue interfaces that have similar intensity values as the needle tip, but are not aligned with the trajectory. Similar to the original RT method, each line also has an associated direction, which is given by an angle θ. However, the output for each angle is an image, which is the main difference from the traditional RT where the output in such a case is a 1D function. If the set of knots along L is given as $(t_1, ..., t_n)$, the value of the new extracted feature is given by:

$$US_{needle}(US_B, L(t)) = \frac{\int_{t_i}^{t_{i+1}} US_B(L(t))dt}{\|L(t_{i+1}) - L(t_i)\|_2}; t \in [t_i, t_{i+1}]. \quad (1)$$

Here, US_B represents the band-pass filtered US image (Fig. 3 (b)). We obtain US_B using the Log-Gabor filter without the orientation selectivity $LG(\omega) = exp(-log(\omega/\kappa)^2/2log(\sigma_\omega)^2)$. L is the line along which features are obtained. The function US_{needle} assigns all the pixels between the knots t_1 and t_{i+1} along L, the mean value of function US_{needle} along L, between the same two knots. Investigating the calculated US_{needle} image we can see that the pixel corresponding to the estimated needle tip is enhanced after this feature extraction operation (Fig. 3 (c)). Fig. 3 (d) shows the overlay of the maximum intensity pixels of US_{needle} (colour coded in red) on the B-mode US image. The needle tip localization was achieved by selecting the first maximum intensity needle tip pixel, lying along the calculated final needle trajectory and outside of US_{ROI}, from the enhanced needle images.

2.2 Data Acquisition and Experiments

The US images used in the evaluation of the proposed method were obtained using an iU22 ultrasound system (Philips Ultrasound, Bothell, WA) with a 2D curvilinear transducer (C5-1). Freshly excised *ex vivo* porcine and bovine tissue samples, obtained from a local butcher, were used as the imaging medium. Standard 17 gauge Tuohy anesthesia needles (Arrow International, Reading, PA, USA) were inserted to this setup. A total of individual 150 2D US images (75 porcine and 75 bovine) were collected where the imaging depth setting varied from 5 cm up to 9 cm. The needle was inserted at different angles ($40° - 70°$), and various insertion depths (2 cm - 9 cm). In all the collected images the insertion angle was steep enough so that the only visible portion of the needle in the collected US image was the end part of the shaft and the needle tip. Quantitative validation was obtained by comparing the segmented needle tip, performed using the proposed method, against the gold standard manual segmentation. The manual segmentation was also confirmed by the known depth at which the

needle was inserted. "The error was calculated by measuring the Euclidean distance (ED) between these points and calculating root-mean-square (RMS) and 95% confidence intervals. The proposed method was implemented in MATLAB. The Log-Gabor filter parameters were automatically optimized using the framework proposed in [9]. For the MLESAC algorithm $\sigma = 1$ provided successful inlier estimation results while avoiding the estimation of unwanted outliers. The angle θ for the needle tip enhancement ranged from $0° - 300°$ with $6°$ increments. Throughout the experimental validation these parameters were not changed.

3 Results

Figure 4 shows sample results. Investigating the B-mode US images, we can see that the proposed method successfully enhances the needle tip in the presence of disconnected and partially visible needle shaft. Due to the directionally optimized local phase features, the proposed method is not affected by the soft tissue interfaces with higher intensity values (Fig. 4 (a) second row). Furthermore, the method appears unaffected by the intensity variations present in different US scans. If the needle shaft has a similar intensity value as the tip the proposed method results in the enhancement of both features (Fig. 4 (a) second row). The processing time in MATLAB was 0.8 seconds for a 450×450 2D image. Needle scans inside the bovine and porcine tissue resulted with an overall mean ED error value of 0.43 mm (RMS 0.53 mm SD 0.31 mm and 95% CI 0.51 mm) and 0.4 mm (RMS 0.49 mm SD 0.29 mm 95% CI 0.47 mm), respectively (Fig. 4 (b)). The maximum localization errors were 1.19 mm and 1.24 mm for bovine and porcine scans, respectively.

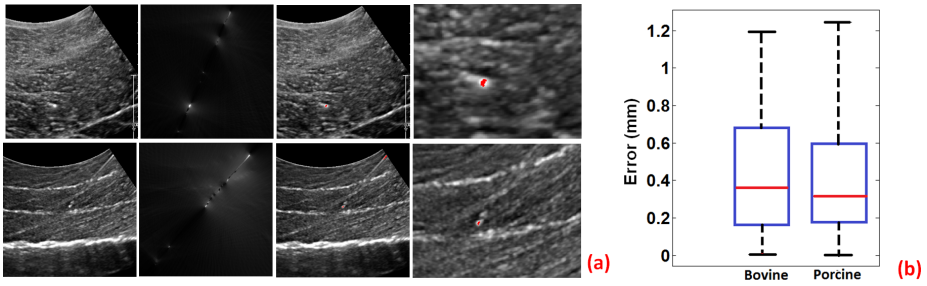

Fig. 4. (a) Sample results of porcine tissue *ex vivo*. First column: B-mode US images. Second column: Result of needle tip enhancement. Third column: Overlay of enhanced needle tip on top of the B-mode US image. Fourth column: Expanded view of the third column.(b) Quantitative results for needle tip localization.

4 Discussions and Conclusions

We propose a method to localize the tip using both echo information from the tip and the partially visible needle shaft. The quantitative experiments indicate

a mean RMS error of 0.53 mm and 0.49 mm for for bovine and porcine tissue respectively. The accuracy of the method is improved using the available prior information before the insertion of the needle. The method is tested on epidural needles with no or minimal bending. For situations where needle bending occurs, tool models incorporating this bending information can be incorporated to the framework. If the US transducer is placed further from the needle, the ROI selection step can be eliminated since for these situations the visible section of the needle shaft would be longer. Future work will focus on validation of the method on *in vivo* scans and different application of image guided interventions where visualization of needles from US data is of importance.

References

[1] Schafhalter-Zoppoth, I., McCulloch, C.E., Gray, A.T.: Ultrasound visibility of needles used for regional nerve block: An in vitro study. Reg. Anes. and Pain Medicine 29(5), 480–488 (2004)
[2] Hatt, C.R., Ng, G., Parthasarathy, V.: Enhanced needle localization in ultrasound using beam steering and learning-based segmentation. Comp. Med. Imag. and Grap. 14, 45–54 (2015)
[3] Zhou, H., Qiu, W., Ding, M., Zhang, S.: Automatic needle segmentation in 3D ultrasound images using 3D improved Hough transform. In: Proc. SPIE Med. Imag., pp. 691821-1-691821-9 (2008)
[4] Ding, M., Fenster, A.: Projection-based needle segmentation in 3D ultrasound images. In: Ellis, R.E., Peters, T.M. (eds.) MICCAI 2003. LNCS, vol. 2879, pp. 319–327. Springer, Heidelberg (2003)
[5] Barva, M., Uhercik, M., Mari, J.M., Kybic, J., Duhamel, J.R., Liebgott, H., Hlavac, V., Cachard, C.: Parallel integral projection transform for straight electrode localization in 3-D ultrasound images. IEEE Trans. UFFC 55(7), 1559–1569 (2008)
[6] Novotny, P.M., Stoll, J.A., Vasilyev, N.V., del Nido, P.J., Dupont, P.E., Howe, R.D.: GPU based real-time instrument tracking with three dimensional ultrasound. Med. Imag. Anal. 11(5), 458–464 (2007)
[7] Uhercik, M., Kybic, J., Liebgott, H., Cachard, C.: Model fitting using ransac for surgical tool localization in 3D ultrasound images. IEEE Trans. on Biomed. Eng. 57(8), 1907–1916 (2010)
[8] Wu, Q., Yuchi, M., Ding, M.: Phase Grouping-Based Needle Segmentation in 3-D Trans-rectal Ultrasound-Guided Prostate Trans-perineal Therapy. Ultrasound in Med. and Biol. 40(4), 804–816 (2014)
[9] Hacihaliloglu, I., Abugharbieh, R., Hodgson, A., Rohling, R.N.: Automatic adaptive parameterization in local phase feature-based bone segmentation in ultrasound. Ultrasound in Med. and Biol. 37(10), 1689–1703 (2011)
[10] Torr, P.H.S., Zisserman, A.: MLESAC: A New Robust Estimator with Application to Estimating Image Geometry. Journal of Computer Vision and Image Under 78(1), 138–156 (2000)
[11] Arias-Castro, E., Donoho, D.L., Huo, X., Tovey, C.: Connect-the-dots: how many random points can a regular curve pass through. Adv. Adv. in Appl. Prob., 37(3), 571–603 (2005)
[12] Kumar, R., Vazquez-Reina, A., Pfister, H.: Radon-Like features and their application to connectomics. In: IEEE CVPR Workshop, pp. 186–193 (2010)